Astron. Astrophys. 361, 92–100 (2000)

ASTRONOMY
AND
ASTROPHYSICS

# High resolution abundance analysis of 16 giants and subgiants in the metal-poor globular cluster NGC 6397⋆

**B.V. Castilho**[1], **L. Pasquini**[2], **D.M. Allen**[1], **B. Barbuy**[1], **and P. Molaro**[3]

[1] Universidade de São Paulo, CP 3386, São Paulo 01060-970, Brazil
[2] European Southern Observatory, Karl-Schwarzschild-Strasse 2, 85748 Garching, Germany
[3] Osservatorio Astronomico di Trieste, Via G.B. Tiepolo 11, 34131 Trieste, Italy

Received 7 April 2000 / Accepted 20 July 2000

**Abstract.** High-resolution échelle spectra of five giants and eleven subgiants of the metal-poor globular cluster NGC 6397 were obtained at the ESO 3.5m (NTT) and 3.6m telescopes.

A detailed analysis of the 16 sample stars was carried out, providing atmospheric parameters ($T_{\rm eff}$, log $g$, [Fe/H], $v_t$) and element abundances.

The metallicity of the cluster is [Fe/H] = $-2.0$ with a r.m.s. of $\pm 0.05$, irrespective of the position in the Colour - Magnitude Diagram, with no variations as a function of effective temperatures and gravities. The dispersion in metal abundance, obtained over a range of 5 magnitudes and 1400 K, is negligible and well within the measurement uncertainties.

$\alpha$-elements are mildly overabundant while the s-elements are deficient relative to iron by about 0.2 dex. [O/Fe] is also mildly overabundant for the two stars where the line is detected.

The Li abundances in the present sample and those of turnoff stars by Pasquini and Molaro (1996) are complementary in terms of evolutionary stage. The Li abundances decrease off the main sequence along the red giant branch, confirming that extra depletion must occur for stars cooler than $\sim$5000 K and V brighter than $\sim$14.

**Key words:** stars: abundances – stars: Hertzsprung–Russell (HR) and C-M diagrams – stars: Population II – Galaxy: globular clusters: individual: NGC 6397 – Galaxy: halo

## 1. Introduction

The metal-poor globular cluster NGC 6397 is the second nearest to us, at a distance of 2.2 kpc. Despite the brightness of its stars, only 11 giants in total have been so far analysed at high resolution by Bell et al. (1979), Gratton (1982, G82), Gratton & Ortolani (1989), Minniti et al. (1993, 1996), Norris & Da Costa (1995) and Carretta & Gratton (1997). In addition to these, Pasquini & Molaro (1996) derived Li abundances for 5 turn-off and subgiant stars.

The somewhat more distant globular cluster 47 Tuc (4.6 kpc) has been far more thoroughly studied in terms of high resolution abundance analysis than NGC 6397, since it is a prototype of a metal-rich cluster ([Fe/H] = $-0.8$, [Z/Z$_\odot$] = $-0.3$, Brown & Wallerstein 1992). Regarding fainter subgiant stars in 47 Tuc, there have been a few studies, such as for example, that by Cannon et al. (1998) for more than a hundred faint stars.

NGC 6397 is interesting because it is among the most metal-poor globular clusters, with [Fe/H] $\approx -2.0$, together with M15 ([Fe/H] $\approx -2.2$), M92 ([Fe/H] $\approx -2.3$), M30 ([Fe/H] $\approx -2.13$), NGC 5053 ([Fe/H] $\approx -2.58$) among a few other ones (Sneden et al. 1991; Zinn & West 1984). No more than a dozen globular clusters in the Galaxy have metallicities [Fe/H] $\lesssim -2.0$.

The determination of accurate abundances in NGC 6397 for a wide range of magnitudes ($10.1 \leq V \leq 15.6$), covering effective temperatures ranging from 4100 to 5500 K, allows us to address several issues:

1) Do variations in chemical composition exist among stars belonging to the same cluster? CNO variations are clearly determined in several clusters, and evidence for heavy element abundance variations is definitely present in objects like Omega Centauri (Pancino et al. 2000 and references therein).

2) Are these possible variations related to the position of the stars in the Colour-Magnitude Diagram (CMD)? This topic is particularly relevant in investigating the presence of processes in stellar interiors, such as diffusion, dredge-up or bottom burning processes.

3) What is the metallicity of a cluster? If indeed we can determine that a single value of metallicity can be assigned to a cluster, then the age can be derived from direct comparison with theoretical evolutionary models (Gratton et al. 1997).

The observations are described in Sect. 2. In Sect. 3 the stellar parameters are derived and in Sect. 4 element abundances are obtained and discussed. A summary is given in Sect. 5.

## 2. Observations

The observations were obtained using the CASPEC spectrograph at the ESO 3.6m telescope and the EMMI spectrograph at the Nasmyth focus of the 3.5m NTT telescope.

*Send offprint requests to*: B.V. Castilho

⋆ Observations collected at the European Southern Observatory – ESO, Chile

**Table 1.** Log of observations

| Star* | V | Exp. (s) | Date | S/N ** | Inst. |
|---|---|---|---|---|---|
| C25 | 12.22 | 3600 | 06/22/93 | 100 | CASPEC |
| C28 | 11.81 | 3000 | 06/22/93 | 100 | CASPEC |
| C43 | 10.94 | 3600 | 06/22/93 | 150 | CASPEC |
| C211 | 10.16 | 2400 | 06/22/93 | 120 | CASPEC |
| C603 | 10.35 | 2400 | 06/22/93 | 150 | CASPEC |
| NO04 | 13.34 | 3600 | 06/05/95 | 45 (80) | EMMI |
| | | 1800 | 08/06/95 | 63 | EMMI |
| NO06 | 13.49 | 1800 | 05/25/96 | 36 (50) | EMMI |
| | | 1800 | 05/25/96 | 38 | EMMI |
| NO08 | 13.18 | 5400 | 06/05/95 | 70 | EMMI |
| NO19 | 14.16 | 2800 | 05/25/96 | 36 (45) | EMMI |
| | | 2400 | 05/26/96 | 30 | EMMI |
| NO20 | 14.40 | 5400 | 06/05/95 | 40 (65) | EMMI |
| | | 3000 | 08/05/95 | 45 | EMMI |
| | | 2420 | 08/05/95 | 42 | EMMI |
| NO25 | 14.71 | 5400 | 06/05/95 | 30 (60) | EMMI |
| | | 5400 | 06/05/95 | 44 | EMMI |
| | | 3000 | 08/05/95 | 39 | EMMI |
| | | 2400 | 08/05/95 | 32 | EMMI |
| NO26 | 14.85 | 3000 | 05/25/96 | 22 (40) | EMMI |
| | | 3000 | 05/25/96 | 22 | EMMI |
| | | 3000 | 05/25/96 | 27 | EMMI |
| NO27 | 14.87 | 5400 | 06/18/96 | 32 (45) | EMMI |
| | | 4200 | 06/18/96 | 26 | EMMI |
| | | 5400 | 06/19/96 | 25 | EMMI |
| NO31 | 15.10 | 5400 | 06/05/95 | 23 (40) | EMMI |
| | | 3600 | 08/06/95 | 35 | EMMI |
| | | 3600 | 08/06/95 | 35 | EMMI |
| | | 3600 | 08/06/95 | 35 | EMMI |
| NO35 | 15.47 | 5400 | 05/25/96 | 33 (45) | EMMI |
| | | 5400 | 05/25/96 | 29 | EMMI |
| | | 5400 | 05/26/96 | 25 | EMMI |
| NO37 | 15.65 | 5400 | 05/26/96 | 23 (35) | EMMI |
| | | 5100 | 05/26/96 | 24 | EMMI |
| | | 5100 | 05/26/96 | 23 | EMMI |

* Star identifications adopted from Anthony-Twarog et al. (1992) (NO) and Cannon et al. (1974) (C);
** S/N measured at the 6700 Å region; in parentheses S/N ratios of combined spectra are given.

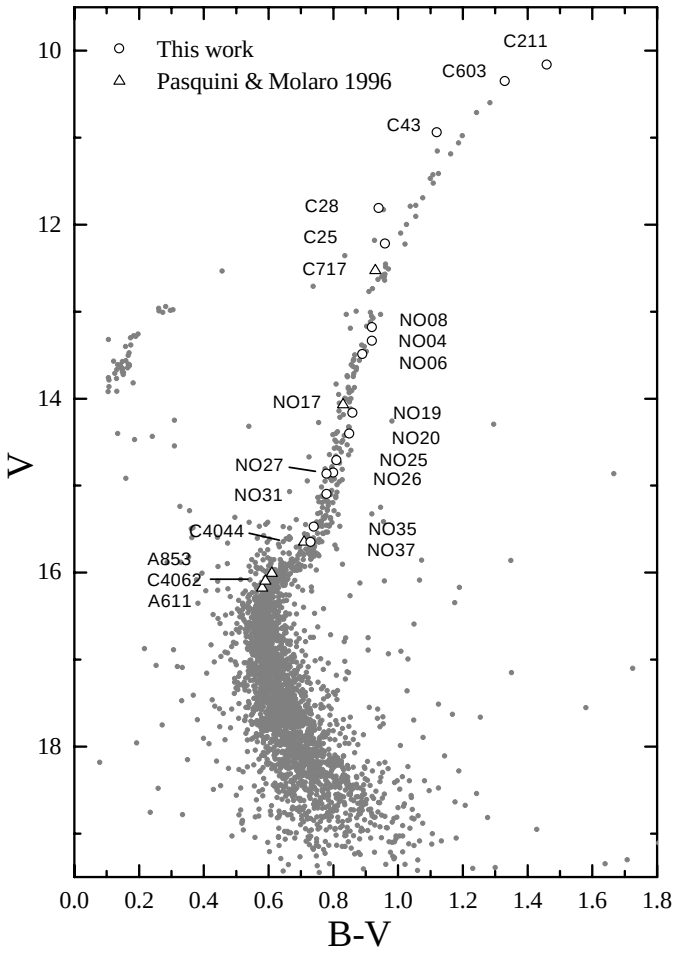


**Fig. 1.** V vs. (B−V) diagram of NGC 6397 by Desidera et al. (1998), where the location of stars studied in the present work (open circles) are indicated, together with those previously studied by Pasquini & Molaro (1996) (open triangles). Identifications 'C', 'NO' and 'A' correspond respectively to Cannon (1974), Anthony-Twarog et al. (1992) and Alcaino et al. (1987).

The Cassegrain Échelle Spectrograph (CASPEC) at the 3.6m was used with a thinned and anti-reflection coated Tektronix CCD of 512×512 pixels, of pixel size 27$\mu$mx27$\mu$m (ESO # 32). The wavelength region covered is $\lambda\lambda$ 5000-7500 Å, at a resolution of R $\approx$ 25,000.

EMMI was used in échelle mode, with grism 6 as crossdisperser providing a spectral coverage of the region $\lambda\lambda$ 6000-8000 Å. With the Tektronix 2040x2048 CCD ESO # 36, and the f/5 Long Camera the dispersion is 0.067 Å/pixel in the 6700 Å region. A slit aperture of 1.2 arcsec gives a resolving power of R $\approx$ 23,000.

The data were reduced using MIDAS and IRAF facilities.

The log of observations is reported in Table 1.

A total of 16 stars were observed in the magnitude range 10.1 $\leq$ V $\leq$ 15.6. This corresponds to effective temperatures ranging from 4100 to 5500 K. In Fig. 1 the program stars are placed on the CCD V vs. (B−V) CMD by Desidera et al. (1998). Note that C28 and C43 might be Asymptotic Giant Branch (AGB) stars from their location in the CMD diagram.

UBV photometry is given in Cannon (1974) and Strömgren photometry in Anthony-Twarog et al. (1992). The stars were chosen to be likely cluster members, either from the inspection of the Cannon (1974) diagrams, or because they were very close to Anthony-Twarog et al.'s fiducial line.

The magnitudes derived by these authors, together with the corresponding dereddened colours, are given in Table 2. A reddening of E(B−V) = 0.18 reported in the compilation by Harris (1996) was adopted.

Radial velocities were measured on the spectra and reported in Table 2.

**Table 2.** Photometric data available for the sample stars (for the subgiants the (B−V) values are derived from (b-y) colours) and heliocentric radial velocities $v_r$ (km $s^{-1}$).

| Giants | $(B-V)_0$ | $(V-K)_0$ | $(J-K)_0$ | ref. | $v_r$ |
|---|---|---|---|---|---|
| C25 | 0.78 | 2.29 | 0.65 | 1,2,3 | 17.0 |
| C28 | 0.77 | 2.18 | 0.63 | 1,3 | 18.5 |
| C43 | 0.95 | 2.61 | 0.72 | 1,2,3 | 18.5 |
| C211 | 1.28 | 3.13 | 0.83 | 1,2,3 | 20.0 |
| C603 | 1.16 | 2.85 | 0.80 | 1,2 | 23.5 |
| Subgiants | $(b-y)_0$ | $(B-V)_0$ | ref. | $v_r$ | |
| NO04 | 0.514 | 0.739 | 4 | 20.0 | |
| NO06 | 0.501 | 0.716 | 4 | 19.5 | |
| NO08 | 0.514 | 0.739 | 4 | 19.5 | |
| NO19 | 0.484 | 0.688 | 4 | 19.5 | |
| NO20 | 0.481 | 0.682 | 4 | 19.5 | |
| NO25 | 0.464 | 0.650 | 4 | 24.5 | |
| NO26 | 0.459 | 0.640 | 4 | 18.0 | |
| NO27 | 0.447 | 0.620 | 4 | 15.0 | |
| NO31 | 0.448 | 0.622 | 4 | 19.5 | |
| NO35 | 0.427 | 0.584 | 4 | 15.5 | |
| NO37 | 0.418 | 0.566 | 4 | 22.5 | |

References: 1) Cannon (1974); 2) Carretta & Gratton (1997); 2) Frogel et al. (1983); 4) Anthony-Twarog et al. (1992)

## 3. Stellar parameters

### *3.1. Temperatures for the giants*

For the 5 cool giants available colours were gathered from the literature, including (B−V), (V−K) and (J−K). We assumed E(V−K) = 2.744E(B−V) and E(J−K) = 0.524E(B−V) (Rieke & Lebofsky 1985). The original (J−K) by Frogel et al. (1983) were given in the CIT system; they were transformed to the Johnson system according to Frogel et al., and these values are given in Table 2. The temperatures were derived using colour-temperature relations by Blackwell et al. (1991, BLP91), McWilliam (1990, M90) based on solar metallicity stars, Gratton et al. (1996, GCC96) for population I stars, and Lejeune et al. (1998, LCB98) and Buser & Kurucz (1992, BK92) for [Fe/H] = −2.0. For the use of the LCB98 relations, the (J−K) colours were transformed to the MSO system according to Bessell & Brett (1988). These temperatures are reported in Table 3 for each of the 5 giants and for each colour and calibration. There is reasonable agreement on effective temperatures derived from the different colours (except B−V) and calibrations.

We adopted as final values the $T_{\rm eff}$ values given by the calibration of (V−K) using LCB98.

### *3.2. Temperatures for the subgiants*

For the subgiants we used the H$\alpha$ profile, employing both the ATLAS and MARCS models, as well as (b−y) Strömgren colours using calibrations by VandenBerg & Bell (1985, VB85) for Z = 0.0003 and 14 Gyr, GCC96 for population I stars, and by transforming (b−y) into (B−V) (cf. VB85, Table 2) and employing the LCB98 colour vs. temperature calibrations for

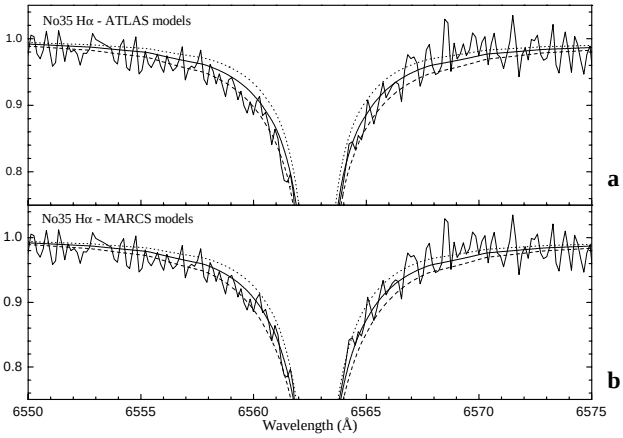


**Fig. 2a and b.** Subgiant NO35: fit of H$\alpha$ profile employing (**a**) ATLAS models for $T_{\rm eff}$ = 5500 K (solid line), 5250 K (dotted line) and 5750 K (dahed line) (**b**) MARCS models for $T_{\rm eff}$ = 5300 K (solid line), 5050 K (dotted line) and 5550 K (dashed line).

[Fe/H] = −2.0. We assume a relation E(b−y) = 0.73 E(B−V) (Crawford & Mandwewala 1976), or E(b−y) = 0.13; note that Anthony-Twarog et al. (1992) adopted E(b−y) = 0.14, whereas Pasquini & Molaro (1996) employed E(b−y) = 0.12. The temperatures obtained for the 11 subgiants are shown in Table 4; it is clear that the discrepancies are very pronounced in this temperature range, and deserve a few comments:

*(a)* The differences between the temperatures derived through H$\alpha$ fitting using MARCS (Gustafsson et al. 1975) or ATLAS with overshooting (Kurúcz 1993) models are rather striking. We used a mean of these two determinations based on H$\alpha$ profiles - Column (4) is a mean of Columns (2) and (3) in Table 4. In Fig. 2 are shown the best fit and the variations of ±250 K with both models, for the subgiant NO35: note that a difference of 200 K is found between the best fits for the two models.

*(b)* The effective temperatures derived from colour vs. temperature calibrations also show discrepancies, due to the differences in the calibrations by GCC96, VB85, LCB98, as shown in Fig. 3.

Final means of $T_{\rm eff}$ values derived from H$\alpha$ (Column (4) of Table 4) and those derived from colours vs. temperatures (Column (8) of Table 4) are adopted and given in Column (9) of Table 4.

### *3.3. Gravities*

The classical relation $\log g_* = 4.44 + 4\log T_*/T_\odot + 0.4(M_{\rm bol} - 4.74) + \log M_*/M_\odot$ was used to derive the stellar gravities (adopting $T_\odot$ = 5770 K, $M_*$ = 0.8 $M_\odot$ and $M_{{\rm bol}\odot}$ = 4.74 cf. Bessell et al. 1998). For deriving $M_{{\rm bol}*}$ we adopted a distance of 2.2 kpc, E(B−V) = 0.18 and bolometric magnitude corrections $BC_V$ by LCB98; the resulting $M_{\rm bol}$ values are given in Table 5.

The ionisation equilibrium with these gravities was checked by verifying if the curves-of-growth of FeI and FeII give the same Fe abundance. Corrections to lower gravities of $\Delta\log g <$ 0.2, and of 0.3 dex for C25 were applied.

**Table 3.** Effective temperatures (K) for the giant stars.

| Star* | $T_{B-V}$ BK92 | $T_{B-V}$ BLP91 | $T_{V-K}$ BLP91 | $T_{B-V}$ M90 | $T_{V-K}$ M90 | $T_{J-K}$ M90 | $T_{B-V}$ LCB98 | $T_{V-K}$ LCB98 | $T_{J-K}$ LCB98 | $T_{B-V}$ GCC96 | $T_{V-K}$ GCC96 | $T_{J-K}$ GCC96 |
|---|---|---|---|---|---|---|---|---|---|---|---|---|
| C25 | 4813 | 5323 | 4850 | 5322 | 4803 | 4722 | 4991 | 4811 | 4688 | 5316 | 4819 | 4751 |
| C28 | 4871 | 5392 | 4933 | 5406 | 4917 | 4782 | 5043 | 4925 | 4789 | 5394 | 4928 | 4809 |
| C43 | 4500 | 4989 | 4556 | 4909 | 4509 | 4523 | 4761 | 4508 | 4457 | 4944 | 4537 | 4557 |
| C211 | 3938 | 4383 | 4222 | 4255 | 4142 | 4238 | 4241 | 4150 | 4239 | 4340 | 4182 | 4274 |
| C603 | 4118 | 4588 | 4394 | 4482 | 4322 | 4314 | 4540 | 4325 | 4296 | 4561 | 4358 | 4350 |

**Table 4.** Effective temperatures (K) for the subgiant stars. Column (4) is a mean of Columns (2) and (3); Column (8) is a mean of Columns (5), (6) and (7); Column (9) is the adopted temperature, which is a mean of Columns (4) (H$\alpha$ based temperature) and (8) ((b−y) based temperature). The $T_{b-y}^{LCB98}$ values were derived by transforming b−y to B−V in order to employ LCB98 relations.

| Star | $T_{(H\alpha)}$ MARCS | $T_{(H\alpha)}$ ATLAS | $T_{(H\alpha)}^{mean}$ | $T_{b-y}$ VB85 | $T_{b-y}$ GCC96 | $T_{b-y}$ LCB98 | $T_{b-y}^{mean}$ | $T^{mean}$ |
|---|---|---|---|---|---|---|---|---|
| (1) | (2) | (3) | (4) | (5) | (6) | (7) | (8) | (9) |
| NO04 | 4700 | 4750 | 4725 | 4885 | 5125 | 5060 | 5023 | 4874 |
| NO06 | 4800 | 5000 | 4900 | 4940 | 5195 | 5120 | 5085 | 4992 |
| NO08 | 4700 | 4750 | 4725 | 4885 | 5120 | 5060 | 5022 | 4873 |
| NO19 | 4900 | 5000 | 4950 | 5020 | 5295 | 5170 | 5162 | 5056 |
| NO20 | 5000 | 5250 | 5125 | 5030 | 5315 | 5200 | 5182 | 5153 |
| NO25 | 5200 | 5500 | 5350 | 5125 | 5410 | 5290 | 5275 | 5313 |
| NO26 | 5100 | 5250 | 5175 | 5150 | 5440 | 5320 | 5303 | 5339 |
| NO27 | 5200 | 5500 | 5350 | 5210 | 5505 | 5370 | 5362 | 5356 |
| NO31 | 5300 | 5500 | 5400 | 5205 | 5505 | 5380 | 5363 | 5382 |
| NO35 | 5300 | 5500 | 5400 | 5310 | 5625 | 5490 | 5475 | 5438 |
| NO37 | 5400 | 5750 | 5575 | 5360 | 5675 | 5520 | 5518 | 5547 |

**Table 5.** Atmospheric parameters adopted for the sample stars.

| Star | $T_{\rm eff}$ | $M_{\rm bol}$ | log $g$ | [Fe/H] | $v_t$ (km s$^{-1}$) |
|---|---|---|---|---|---|
| C25 | 4810 | −0.50 | 1.60 | −2.00 | 1.9 |
| C28 | 4920 | −0.87 | 1.60 | −2.00 | 2.2 |
| C43 | 4510 | −1.94 | 1.20 | −2.10 | 2.0 |
| C211 | 4150 | −3.04 | 0.60 | −2.10 | 2.2 |
| C603 | 4320 | −2.68 | 0.90 | −2.00 | 1.8 |
| NO04 | 4875 | 0.535 | 2.10 | −2.05 | 1.4 |
| NO06 | 4990 | 0.717 | 2.20 | −2.00 | 1.4 |
| NO08 | 4875 | 0.376 | 2.10 | −2.00 | 1.3 |
| NO19 | 5055 | 1.410 | 2.55 | −1.95 | 1.2 |
| NO20 | 5155 | 1.664 | 2.70 | −1.95 | 1.2 |
| NO25 | 5310 | 1.993 | 2.80 | −1.95 | 1.2 |
| NO26 | 5340 | 2.147 | 2.90 | −2.00 | 1.2 |
| NO27 | 5355 | 2.176 | 3.00 | −2.00 | 1.2 |
| NO31 | 5380 | 2.408 | 3.10 | −1.90 | 1.2 |
| NO35 | 5440 | 2.737 | 3.20 | −2.00 | 1.2 |
| NO37 | 5545 | 2.924 | 3.30 | −2.00 | 1.1 |

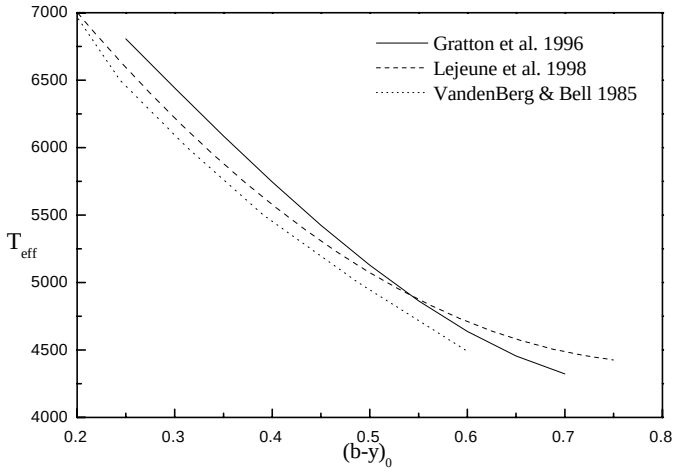


**Fig. 3.** Calibration of effective temperature $T_{\rm eff}$ vs. $(b-y)_o$ by Gratton et al. (1996), Lejeune et al. (1998) and VandenBerg & Bell (1985).

### *3.4. Metallicity*

In Table 6 are reported the metallicities attributed to NGC 6397 in the literature, where most values remain in the range $-2.0 <$ [Fe/H] $< -1.8$.

The metallicities of the program stars were determined using curves of growth of FeI lines where the updated code RENOIR by M. Spite was employed. We have adopted FeI and FeII oscillator strengths log gf by Wiese et al. (1969). These give metallicities very similar to those obtained by employing oscillator strengths given in Spite et al. (1987) or by our fittings to the solar spectrum (Barbuy et al. 1999), whereas by using oscillator strengths by Carretta & Gratton (1997) the derived metallicities are down by 0.1 dex, with [Fe/H] = −2.1. In Figs. 4a,b the FeI and FeII curves-of-growth for the giant C603 are shown, using

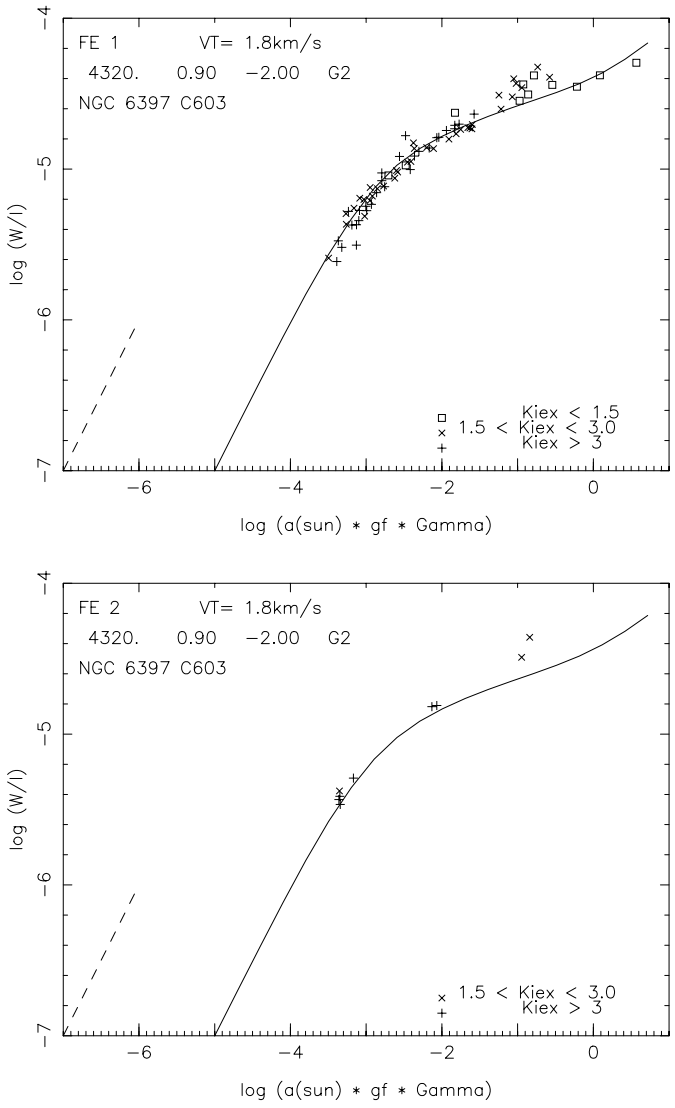


**Fig. 4.** Curves of growth of FeI and FeII lines for the star C603, employing oscillator strengths by Wiese et al. (1969).

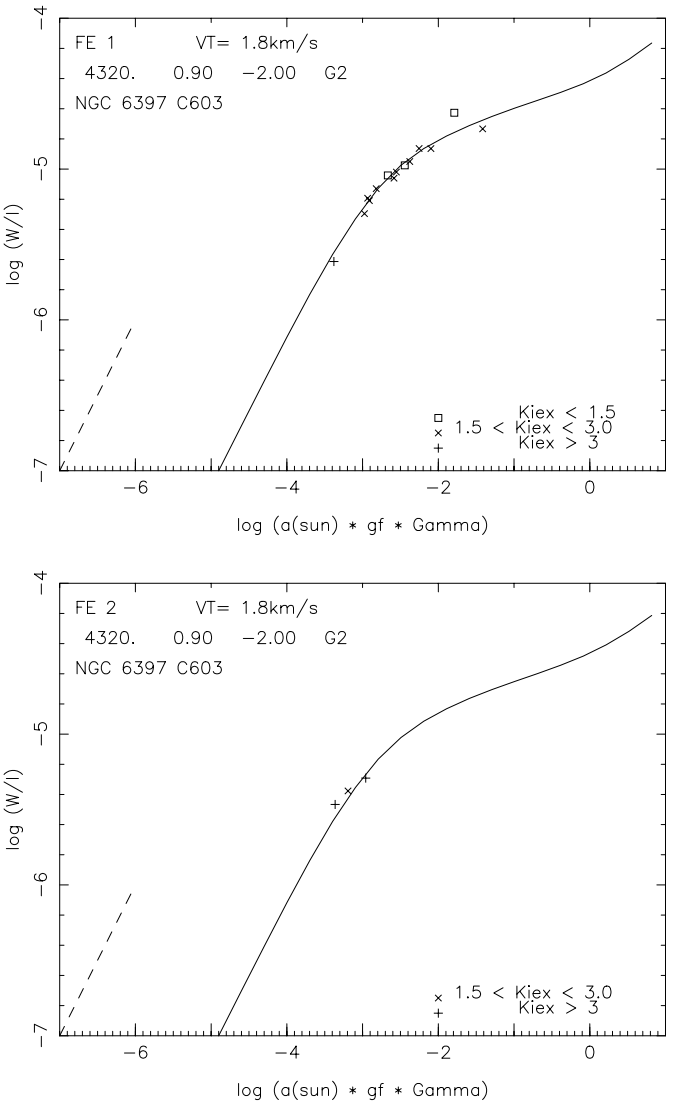


**Fig. 5.** Curves of growth of FeI and FeII lines for the star C603, employing oscillator strengths by Carretta & Gratton (1997).

gf-values of Wiese et al. (1969), and in Figs. 5a,b the curves-of-growth using gf-values of Carretta & Gratton (1997).

In Fig. 6 the FeI combined with the FeII curves of growth for the subgiant NO04 are shown. Microturbulence velocities $v_t$ were also determined from the curves of growth.

Curves of growth built with MARCS and ATLAS models for the giant C43 with $T_{eff}$ = 4500 K and the subgiant NO37 with $T_{eff}$ = 5500 K give essentially the same metallicity, showing good agreement between the two sets of models for metallicity determination in these metal-poor stars.

For the subgiants the adopted $T_{eff}$ values are close to those derived using the VB85 (b−y) vs. effective temperature relations. If GCC96 $T_{eff}$s were used, the derived metallicities would be ∼0.2 dex higher (a 100K increase in $T_{eff}$ corresponds to a 0.1 dex increase in metallicity, in the range of atmospheric parameters of our program stars).

Table 5 shows the stellar parameters $T_{eff}$, log $g$, [Fe/H] and $v_t$. We obtain a mean metallicity of [Fe/H] = −2.0.

## 4. Element abundances

Spectrum synthesis calculations were used to fit the observed spectra line-by-line, as listed in Tables 8 and 9.

The calculations of synthetic spectra were carried out using a revised version of the code described in Barbuy (1982) where molecular lines of CN $A^2\Pi$-$X^2\Sigma$, $C_2$ Swan $A^3\Pi$-$X^3\Pi$ and TiO $A^3\Phi$-$X^3\Delta$ $\gamma$ system are taken into account.

The oscillator strengths adopted are indicated in Table 9. We used the laboratory oscillator strengths by Fuhr et al. (1988), Martin et al. (1988), Wiese et al. (1969), or when these were not available, those given by Spite et al. (1987) or Barbuy et al. (1999).

The MARCS photospheric models for giants of Gustafsson et al. (1975), and their grid extensions kindly made available to us were employed.

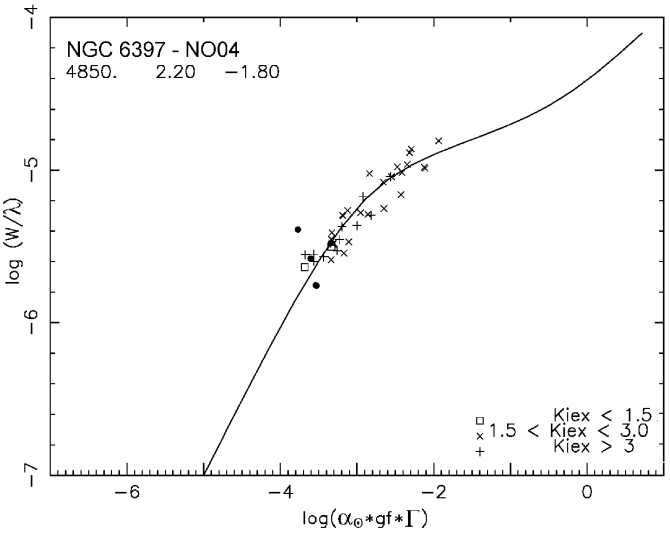


**Fig. 6.** Curve of growth of FeI and FeII (black dots) lines for the star NO04

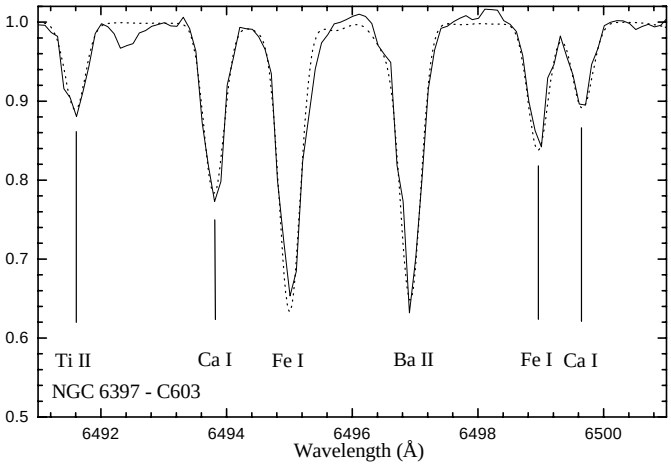


**Fig. 7.** Observed spectrum of C603 (——) and synthetic spectrum (- - - -) in a region containing FeI, TiII, CaI, and BaII lines.

**Table 6.** Metallicity values assigned to NGC 6397 in the literature.

| [M/H] | reference | method |
|---|---|---|
| −2.02 | 1 | a |
| −1.91 | 2 | a |
| −1.91 | 3 | a |
| −2.24 | 4 | b |
| −1.91 | 5 | b |
| −1.67 | 6 | c |
| −1.58/−1.65 | 7 | d |
| −1.85 | 8 | e |
| −1.94 | 9 | f |
| −1.82 | 9 | f |
| −2.0 | 10 | g |
| −2.21 | 11 | g |
| −2.2 | 12 | g |
| −1.88 | 13 | g |
| −1.99 | 14 | g |
| −2.03 | 15 | g |
| −1.81 | 16 | g |

References to Table: 1 Webbink (1985); 2 Djorgovski (1993); 3 Harris (1996); 4 Zinn (1980); 5 Zinn & West (1984); 6 Bica & Pastoriza (1983); 7 Ardeberg et al. (1983); 8 Caldwell & Dickens (1988); 9 Rutledge et al. (1997); 10 Bell et al. (1979); 11 Gratton (1982); 12 Pilachowski et al. (1983); 13 Gratton & Ortolani (1989); 14 Minniti et al. (1993); 15 Norris & Da Costa (1995); 16 Carretta & Gratton (1997). Method employed: a: compilation; b: integrated Q39 photometry; c: integrated DDO photometry; d: Strömgren and BV photometry; e: spectrum synthesis of giants at λλ 4060-4370 Å; f: medium resolution spectroscopy; g: high resolution spectroscopy.

### *4.1. α-elements*

Fig. 7 shows a region containing lines of TiII, CaI and BaII lines in C603 and the corresponding computed synthetic spectrum, illustrating that the fits achieved for the giants are satisfactory.

It can be seen in Table 7 that $\alpha$-elements are overabundant with [Ca/Fe] $\approx$ [Si/Fe] $\approx$ 0.2 and [Ti/Fe] $\approx$ 0.4. Also, [O/Fe] $\approx$ 0.15, similar to the mean obtained by Minniti et al. (1996) who found however strong variations ($0.04 <$ [O/Fe] $< 0.44$) for their 5 stars; for C603, in common with the present work, Minniti et al. found [O/Fe] = 0.21, similar to our value of [O/Fe] = 0.15. Gratton (1982) obtained a mean of [O/Fe] = 0.5, which was revised by Pilachowski et al. (1983) taking into account carbon deficiencies, and corrected to [O/Fe] = +0.27, also similar to our result. This [O/Fe] value is low compared to that for field stars, where [O/Fe] $\approx$ 0.5 using the [O I] $\lambda$6300 Å line (e.g. Barbuy 1988; Carretta et al. 2000), but in good agreement with values found in other clusters (Kraft et al. 1993, Table 7).

The values of $\alpha$-elements show some variations from star to star of $\Delta$[X/Fe] $\leq$ 0.25. These values are essentially consistent with those for M 3 and M 13 by Kraft et al. (1993), also reported in Table 7.

### *4.2. s-elements*

We determine the abundances of Y and Ba for the giants and Ba for the subgiants. For all stars these $s$-elements show a deficiency relative to Fe, as expected for such an old cluster.

### *4.3. Lithium abundances*

The lithium abundances are derived by fitting synthetic spectra to the observed LiI $\lambda$6707.8 Å line. Note that the intensity of Li lines are very sensitive to effective temperatures (Castilho et al. 2000). The Li lines are weak as shown in Fig. 8 for the subgiant NO20. For the cases where the Li line was not detected, we used the S/N $2\sigma$ level to estimate an upper limit for the Li abundance. The NLTE corrections according to Carlsson et al. (1994) are of second order ($<$0.03 dex). A clear decrease of the Li abundance with effective temperature is seen in Table 7 and Fig. 9.

Subgiant stars are cooler than the Spite plateau and dilution of Li is expected. According to Deliyannis et al. (1990) a star of 0.775 $M_\odot$, Z=$10^{-4}$ and mixing length parameter $\alpha$ = 1.5 should show a dilution curve which from an initial value of

**Table 7.** Element abundances obtained for the program stars. The number of lines used to determine the element abundance is indicated in parentheses. Mean abundances obtained for each element are given, and compared to mean values for 2 stars of NGC 6397 by G82 and 5 stars by Minniti et al. (1996) as well as to M3 (7 stars) and M13 (22 stars) by Kraft et al. (1993).

| Star | N(Li) | [O/Fe] | [Na/Fe] | [Si/Fe] | [Ca/Fe] | [Ti/Fe] | [Y/Fe] | [Ba/Fe] |
|---|---|---|---|---|---|---|---|---|
| C25 | 0.52 | – | 0.00(1) | 0.40(1) | 0.10 (9) | 0.27 (9) | −0.41(1) | −0.50(2) |
| C28 | 0.62 | – | 0.30(2) | 0.10(3) | 0.07 (9) | 0.41 (8) | −0.41(1) | −0.22(3) |
| C43 | 0.15 | – | 0.20(2) | 0.38(3) | 0.14(10) | 0.52(10) | −0.10(1) | −0.13(3) |
| C211 | −0.54 | 0.15(1) | 0.30(2) | 0.27(4) | 0.22(11) | 0.32(14) | −0.10(1) | −0.15(3) |
| C603 | −0.30 | 0.15(1) | 0.15(2) | 0.22(4) | 0.26(11) | 0.42(14) | 0.20(1) | −0.03(3) |
| NO04 | 0.75 | – | – | – | 0.22(13) | 0.22 (3) | – | −0.15(2) |
| NO06 | 0.90 | – | – | – | 0.22(10) | <0.4(4) | – | 0.00(2) |
| NO08 | <0.7 | – | – | – | 0.26 (9) | <0.4(4) | – | −0.05(2) |
| NO19 | 1.05 | – | – | – | 0.21 (9) | <0.5(4) | – | −0.17(2) |
| NO20 | 1.15 | – | – | – | 0.30(13) | <0.6(4) | – | −0.22(2) |
| NO25 | 1.30 | – | – | – | 0.31 (7) | <0.6(4) | – | −0.22(2) |
| NO26 | <1.4 | – | – | – | 0.19 (6) | <0.5(4) | – | −0.05(2) |
| NO27 | <1.5 | – | – | – | 0.27 (7) | <0.6(4) | – | −0.12(2) |
| NO31 | 1.55 | – | – | – | 0.17 (9) | – | – | −0.10(2) |
| NO35 | <1.7 | – | – | – | 0.16 (8) | – | – | −0.17(2) |
| NO37 | <1.9 | – | – | – | 0.18 (6) | – | – | −0.25(2) |
| mean | | 0.15 | 0.19 | 0.27 | 0.20 | 0.43 | −0.16 | −0.16 |
| NGC 6397 | (G82) | 0.50 | 0.30 | 0.30 | 0.50 | 0.40 | −0.30 | −0.1 |
| NGC 6397 | (Minniti et al.) | 0.17 | −0.04 | – | – | – | – | – |
| M3 | (Kraft et al.) | −0.02 | −0.07 | 0.24 | 0.33 | – | – | – |
| M13 | (Kraft et al.) | 0.19 | 0.10 | 0.24 | 0.29 | – | – | – |

**Table 8.** Line-by-line element abundances [X/Fe] obtained for the subgiant stars.

| Element | λ (Å) | log gf | NO04 | NO06 | NO08 | NO19 | NO20 | NO25 | NO26 | NO27 | NO31 | NO35 | NO37 |
|---|---|---|---|---|---|---|---|---|---|---|---|---|---|
| CaI | 6102.727 | −0.890 | 0.20 | 0.10 | 0.36 | 0.59 | 0.47 | 0.35 | 0.44 | 0.20 | 0.27 | 0.42 | 0.13 |
| CaI | 6122.226 | −0.409 | 0.64 | 0.50 | 0.55 | 0.27 | – | 0.39 | – | – | 0.25 | 0.22 | – |
| CaI | 6161.295 | −1.050 | 0.18 | – | – | – | 0.48 | – | – | – | 0.44 | – | – |
| CaI | 6162.173 | −0.218 | 0.14 | 0.42 | 0.42 | 0.54 | 0.32 | – | 0.45 | 0.41 | 0.51 | 0.22 | – |
| CaI | 6166.440 | −0.980 | 0.30 | – | 0.36 | – | 0.65 | – | – | – | – | – | – |
| CaI | 6169.044 | −0.550 | 0.14 | 0.16 | – | – | −0.19 | 0.37 | 0.39 | – | −0.14 | – | – |
| CaI | 6169.564 | −0.270 | 0.12 | 0.08 | −0.01 | 0.02 | −0.02 | 0.47 | – | – | −0.16 | – | 0.20 |
| CaI | 6439.075 | 0.470 | 0.14 | 0.62 | 0.12 | −0.10 | 0.34 | 0.37 | – | 0.09 | 0.11 | 0.02 | 0.18 |
| CaI | 6449.808 | −0.550 | 0.22 | 0.46 | 0.21 | 0.14 | 0.06 | – | 0.22 | – | 0.09 | 0.26 | – |
| CaI | 6455.605 | −1.280 | 0.17 | – | – | – | – | – | – | – | – | – | – |
| CaI | 6462.567 | 0.310 | 0.59 | – | – | 0.05 | 0.51 | – | – | 0.38 | 0.40 | 0.26 | – |
| CaI | 6471.668 | −0.590 | 0.58 | – | – | – | – | – | – | – | – | – | – |
| CaI | 6493.781 | 0.140 | 0.05 | 0.14 | 0.13 | 0.16 | −0.03 | 0.01 | −0.21 | 0.24 | 0.13 | 0.06 | 0.13 |
| CaI | 6499.654 | −0.590 | 0.25 | 0.14 | 0.11 | – | −0.07 | – | – | 0.28 | – | −0.03 | – |
| CaI | 6717.687 | −0.610 | −0.10 | 0.09 | – | 0.08 | −0.05 | 0.31 | −0.06 | 0.27 | – | – | – |
| BaII | 6141.720 | −0.077 | -0.20 | 0.00 | 0.00 | −0.15 | −0.25 | −0.20 | −0.10 | −0.25 | −0.10 | −0.10 | −0.30 |
| BaII | 6496.900 | −0.377 | −0.10 | 0.00 | −0.10 | −0.20 | −0.20 | −0.25 | 0.00 | 0.00 | −0.10 | −0.25 | −0.20 |

N(Li) = 2.2 at $T_{\rm eff}$ = 5600 K decreases to about N(Li) = 1.0 at $T_{\rm eff} \approx$ 5200 K, remaining rather constant afterwards. As shown in Fig. 9 the subgiants hotter than 5000 K have detectable Li and their abundances conform rather well to the dilution behaviour. At lower temperatures we have no Li detections and all our upper limits are much lower than dilution predictions suggesting the presence of a destruction mechanism for Li. Note that a 5000 K temperature corresponds to V $\sim$ 13.49 (star NO06, logN(Li) = 0.90) and at V = 13.18 we see an upper limit of logN(Li) $<$ 0.7. The observations of Pilachowski et al. (1993), also shown in Fig. 9, and those of Ryan & Deliyannis (1998) show the same pattern. The only exception is the tidally locked binary HD 89499, with the relatively high Li abundance (N(Li) = 1.4) and $T_{\rm eff}$ = 4875 K.

Charbonnel (1995) has proposed that the mechanism responsible for the Li destruction may be rotational mixing on the giant branch, which is currently invoked to explain also the drop in the $^{12}C/^{13}C$ ratio observed in the same type of stars.

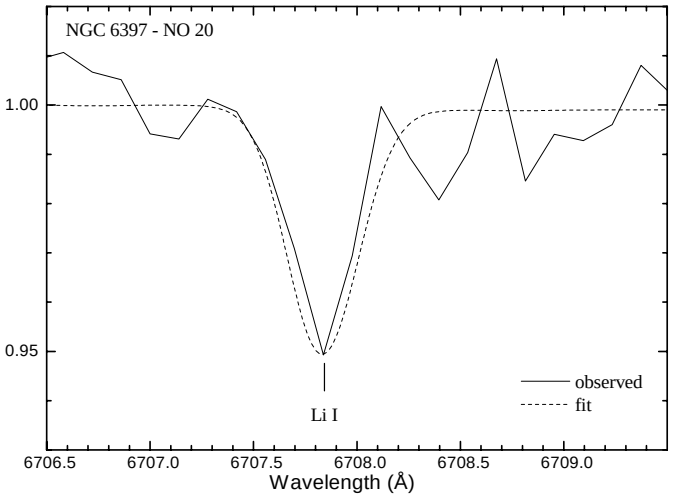


**Fig. 8.** Best fit of the LiI $\lambda$ 6707.8 Å line, with log N(Li) = 1.15, for the star NO20

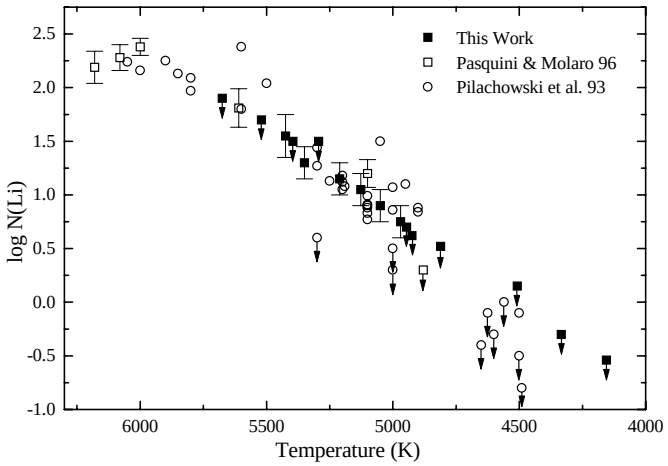


**Fig. 9.** Li abundances vs. $T_{\rm eff}$ for the NGC 6397 stars (filled squares, this work; open squares, Pasquini & Molaro 1996), and a subsample of field metal-poor subgiants from Pilachowski et al. (1993) (open circles). The arrows mean upper limit values.

## 5. Summary

We have carried out a detailed analysis of 16 giants and subgiants of the metal-poor globular cluster NGC 6397. A mean metallicity of [Fe/H]= $-2.0$ was obtained, with small differences with evolutionary stage. This result also shows the homogeneity of the analysis for the wide range of stellar parameters. A detailed study of different calibrations of effective temperatures has shown that the derivation of metallicities is subject to the choice of temperature scale, and in particular for the subgiants there are strong discrepancies between different calibrations. It is clear that the use of Gratton et al.'s (1996) temperature scale would lead to [Fe/H] = $-2.0$ for the giants and $-1.8$ for the subgiants (or [Fe/H] = -2.1 and -1.9 if Gratton et al.'s gf-values are employed), which seems unlikely in terms of stellar evolution.

Li abundances decrease off the main sequence as expected, similarly to metal-poor field stars (Pilachowski et al. 1993).

**Table 9.** Line-by-line element abundances [X/Fe] obtained for the giants.

| Species | $\lambda$ (Å) | log gf | C25 | C28 | C43 | C211 | C603 |
|---|---|---|---|---|---|---|---|
| OI | 6300.311 | −9.750 | – | – | – | 0.15 | 0.15 |
| NaI | 5682.647 | −0.670 | – | 0.30 | 0.30 | 0.30 | 0.10 |
| NaI | 5688.217 | −0.420 | 0.00 | 0.30 | 0.10 | 0.30 | 0.20 |
| MgI | 5528.418 | −0.480 | 0.45 | 0.30 | 0.40 | 0.55 | 0.90 |
| MgI | 5711.095 | −1.300 | 0.00 | −0.10 | −0.20 | 0.00 | 0.00 |
| AlI | 6696.032 | −1.343 | 0.40 | – | – | 0.60 | 0.60 |
| AlI | 6698.669 | −1.650 | – | 0.70 | 0.90 | 0.70 | 0.70 |
| SiI | 5665.563 | −1.740 | – | 0.00 | – | 0.20 | 0.10 |
| SiI | 5708.405 | −1.150 | – | – | 0.30 | 0.20 | 0.10 |
| SiI | 5772.149 | −1.380 | – | 0.10 | 0.25 | 0.20 | 0.10 |
| SiI | 5948.548 | −1.240 | 0.40 | 0.10 | 0.60 | 0.50 | 0.50 |
| CaI | 5588.764 | 0.210 | – | – | 0.20 | 0.40 | 0.40 |
| CaI | 6102.727 | −0.890 | 0.30 | 0.40 | 0.40 | 0.40 | 0.40 |
| CaI | 6122.226 | −0.409 | 0.10 | 0.10 | 0.40 | 0.30 | 0.50 |
| CaI | 6162.180 | −0.218 | 0.00 | 0.00 | 0.20 | 0.40 | 0.30 |
| CaI | 6169.044 | −0.550 | 0.00 | −0.10 | −0.10 | 0.00 | 0.00 |
| CaI | 6169.564 | −0.270 | 0.00 | −0.10 | −0.10 | 0.00 | 0.00 |
| CaI | 6439.083 | 0.470 | 0.20 | 0.10 | 0.20 | 0.30 | 0.55 |
| CaI | 6471.668 | −0.590 | 0.10 | 0.30 | 0.20 | 0.40 | 0.30 |
| CaI | 6499.654 | −0.590 | 0.00 | −0.20 | −0.20 | −0.10 | −0.10 |
| CaI | 6572.795 | −4.290 | – | – | – | 0.00 | 0.10 |
| CaI | 6717.687 | −0.610 | 0.20 | 0.10 | 0.20 | 0.30 | 0.30 |
| TiI | 5866.461 | −0.840 | 0.30 | – | – | 0.20 | 0.30 |
| TiI | 5918.554 | −1.460 | – | 0.90 | 0.50 | 0.20 | 0.40 |
| TiI | 5922.123 | −1.466 | 0.80 | – | 0.50 | 0.20 | 0.40 |
| TiI | 5941.764 | −1.510 | – | – | 0.60 | 0.10 | 0.30 |
| TiI | 6091.177 | −0.423 | – | – | – | 0.30 | 0.30 |
| TiI | 6126.224 | −1.425 | 0.30 | – | – | 0.20 | 0.20 |
| TiI | 6599.113 | −2.085 | – | – | 0.50 | 0.30 | 0.30 |
| TiI | 6743.127 | −1.630 | 0.20 | 0.40 | – | 0.10 | 0.00 |
| TiII | 5154.075 | −1.920 | 0.30 | 0.30 | 0.90 | 1.00 | 1.00 |
| TiII | 5336.794 | −1.700 | 0.20 | 0.30 | 0.50 | 0.30 | 0.70 |
| TiII | 5381.028 | −2.080 | 0.00 | 0.40 | 0.50 | 0.40 | 0.50 |
| TiII | 5418.775 | −2.120 | 0.20 | 0.10 | 0.40 | 0.50 | 0.70 |
| TiII | 6491.582 | −2.100 | 0.20 | 0.30 | 0.30 | 0.30 | 0.30 |
| TiII | 6559.576 | −3.363 | – | 0.60 | 0.50 | 0.50 | 0.50 |
| YII | 5087.426 | −0.170 | −0.40 | −0.40 | −0.10 | −0.10 | 0.20 |
| BaII | 5853.688 | −0.700 | – | −0.25 | −0.10 | −0.05 | −0.20 |
| BaII | 6141.727 | −0.077 | −0.50 | −0.20 | −0.20 | −0.20 | 0.00 |
| BaII | 6496.910 | −0.377 | −0.50 | −0.20 | −0.10 | −0.20 | 0.10 |

$\alpha$-elements are mildly overabundant with [Ca/Fe] $\approx$ [Si/Fe] $\approx$ 0.2 and [Ti/Fe] $\approx$ 0.4. The s-elements Y and Ba are deficient by about 0.2 dex. [O/Fe] is also mildly overabundant by 0.15 dex in agreement with literature values. These overabundances are lower than those predicted by chemical evolution models and the overabundances found in field halo stars (e.g. Chiappini et al. 1999).

*Acknowledgements.* We are grateful to S. Ortolani and S. Desidera for making available the V vs. (B−V) data of NGC 6397. We thank Pamela Bristow of ESO for a revision of the manuscript. We acknowledge partial financial support from the Brazilian agencies CNPq and Fapesp, and ESO. BC acknowledges the FAPESP PhD and post-doc fellowships n$^{\rm o}$ 97/007814-4 and n$^{\rm o}$ 99/05282-5. DMA acknowledges a CNPq Master fellowship.

## References


Alcaino G., Buonanno R., Caloi V., et al., 1987, AJ 94, 917
Anthony-Twarog B.J., Twarog B., Suntzeff N.B., 1992, AJ 103, 1264
Ardeberg A., Lindgren, H., Nissen P.E., 1983, A&A 128, 194
Barbuy B., 1982, PhD Thesis, Univ. Paris VII
Barbuy B., 1988, A&A 191, 121
Barbuy B., Renzini A., Ortolani S., Bica E., 1999, A&A 341, 539
Bell R.A., Dickens R.J., Gustafsson B., 1979, ApJ 229, 604
Bessell M.S., Brett J.M., 1988, PASP 100, 1134
Bessell M.S., Castelli F., Plez B., 1998, A&A 333, 231
Bica E., Pastoriza M., 1983, ASSci 91, 99
Blackwell D.E., Lynas-Gray A.E., Petford A.D., 1991, A&A 245, 567 (BLP91)
Brown J.A., Wallerstein G., 1992, AJ 104, 1818
Buser R., Kurucz R., 1992, A&A 264, 557 (BK92)
Caldwell S.P., Dickens R.J., 1988, MNRAS 234, 87
Cannon R.D., 1974, MNRAS 167, 551
Cannon R.D., Croke B.F.W., Bell R.A., Hesser J.E., Stathakis R.A., 1998, MNRAS 298, 601
Carlsson M., Rutten R.J., Bruls J.H.M.J., Shchukina N.G., 1994, A&A 288, 860
Carretta E., Gratton R.G., 1997, A&AS 121, 95
Carretta E., Gratton R.G., Sneden C., 2000, A&A 356, 238
Castilho B.V., Gregorio-Hetem J., Barbuy B., Spite M., Spite F., 2000, submitted
Charbonnel C., 1995, ApJ 453, L41
Chiappini C., Matteucci F., Beers T.C., Nomoto K., 1999, ApJ 515, 226
Crawford D.L., Mandwewala N., 1976, PASP 88, 917
Desidera S., Bertelli G., Ortolani S., 1998, Poster proceedings of IAU Symp. 189, p. 164
Deliyannis C.P., Demarque P., Kawaler S.D., 1990, ApJS 73, 21
Djorgovski S., 1993, ASP Conf. Ser. 50, p. 373
Frogel J.A., Persson S.E., Cohen J.G., 1983, ApJS 53, 713
Fuhr J.R., Martin G.A., Wiese W.L., 1988, Atomic Transition Probabilities: Iron through Nickel. Journal of Physical and Chemical Reference Data vol. 17, suppl. no. 4
Gratton R.G., 1982, A&A 115, 171 (G82)
Gratton R.G., Ortolani S., 1989, A&A 211, 41
Gratton R.G., Carretta E., Castelli, F., 1996, A&A 314, 191 (GCC96)
Gratton R.G., Fusi Pecci F., Carretta E., et al., 1997, ApJ 491, 749
Gustafsson B., Bell R.A., Eriksson K., Nordlund Å., 1975, A&A 42, 407
Harris W.E., 1996, AJ 112, 1487
Kraft R.P., Sneden C., Langer G.E., Shetrone M.D., 1993, AJ 106, 1490
Kurucz R.L., 1993 CD-ROM No 11, 13,18
Lejeune T., Cuisinier F., Buser R., 1998, A&AS 130, 65
Martin G.A., Fuhr J.R., Wiese W.L., 1988, Atomic Transition Probabilities: Scandium through Manganese. Journal of Physical and Chemical Reference Data vol. 17, suppl. no. 3
McWilliam A., 1990, ApJS 74, 1075
Minniti D., Geisler D., Peterson R.C., Clariá J.J., 1993, ApJ 413, 548
Minniti D., Peterson R.C., Geisler D., Clariá J.J., 1996, ApJ 470, 953
Norris J., Da Costa G.S., 1995, ApJ 447, 680
Pasquini L., Molaro P., 1996, A&A 307, 761
Pancino E., Ferraro F.R., Bellazzini M., Piotto G., Zoccali M., 2000, ApJ, 534, L83
Pilachowski C.A., Sneden C., Wallerstein G., 1983, ApJS 52, 241
Pilachowski C.A., Sneden C., Booth J., 1993, ApJ 407, 699
Rieke G.H., Lebofsky M.J., 1985, ApJ 228, 618
Rutledge G.A., Hesser J.E., Stetson P.B., 1997, PASP 109, 907
Ryan S.G., Deliyannis C.P., 1998, ApJ 500, 398
Sneden C., Kraft R.P., Prosser C.F., Langer G.E., 1991, AJ 102, 2001
Spite M., Huille S., François P., Spite F., 1987, A&AS 71, 591
VandenBerg D.A., Bell R.A., 1985, ApJS 58, 561
Webbink R.F., 1985, In: Goodman J., Hut P. (eds.) IAU Symp. 113, Reidel, Dordrecht, p. 541
Wiese W.L., Martin G.A., Fuhr J.R., 1969, Atomic Transition Probabilities: Sodium through Calcium. NSRDS-NBS 22
Zinn R., 1980, ApJS 42, 19
Zinn R., West W.J., 1984, ApJS 55, 45